Eur. Phys. J. E (2012) **35**: 57
DOI 10.1140/epje/i2012-12057-2

THE EUROPEAN PHYSICAL JOURNAL E

Regular Article

Skin formation and bubble growth during drying process of polymer solution

S. Arai[a] and M. Doi

Graduate School of Engineering, The University of Tokyo, Tokyo, Japan 113-8656

Received 24 March 2012 and Received in final form 6 June 2012
Published online: 11 July 2012 –

Abstract. When a polymer solution with volatile solvent is dried, skins are often formed at the surface of the solution. It has been observed that after the skin is formed, bubbles often appear in the solution. We conducted experiments to clarify the relation between the skin formation and the bubble formation. We measured the time dependence of the thickness of the skin layer, the size of the bubbles, and the pressure in the solution. From our experiments, we concluded that i) the gas in the bubble is a mixture of solvent vapor and air dissolved in the solution, ii) the bubble nucleation is assisted by the pressure decrease in the solution covered by the skin layer, and iii) the growth of the bubbles is diffusion limited, mainly limited by the diffusion of air molecules dissolved in the solution.

1 Introduction

The drying of polymer solutions is an important process in many technologies, such as coating, film making and printing. It is well known that the drying condition is quite important in the process. Without careful control of the drying condition, one often gets troubles in the resulting products.

A source of such troubles is the skin layers formed at the surface of polymer solutions. As the solvent evaporates from polymer solutions, the polymer concentration near the surface becomes high, and polymers often form a layer which has distinctively different rheological property from that of bulk solution. The layer is called skin. The skin layer is considered to be an elastic membrane though the detailed rheological study has not been done.

It is known that once such skin layer is formed, it creates various problems. For example the surface of the dried polymer films is not flat; dimples and wrinkles often appear and bubbles remain trapped in the film.

Despite the importance of the skin layer in the applications, not many scientific studies have been done on the skin layers. de Gennes [1] first discussed the theoretical model for the skin layer (he called it crust). Okuzono *et al.* [2] gave a condition for the skin layer to be formed. Experimentally, Pauchard and Allain [3,4] studied various dimple patterns formed in the drying droplets. Kajiya *et al.* [5] discussed the effect of skin layer formation in the coffee stain problem [6] of polymer solutions. However, there still remain many open questions, *e.g.*, how thick the skin layer is, and how it grows in time, how it changes the rheological properties of the surface [7], and how it affects the drying speed, etc.

The previous studies of the skin layer was focused on the deformation of the solution surface caused by the skins such as dimples and wrinkles [3–5]. In this paper we focus on another important aspect of the troubles caused by the skins, *i.e.*, bubble formation.

It has been known that when polymer solutions are dried quickly, bubbles often appear in the solution and remain trapped in the final product. The question we address here is why the bubbles are formed and how they are related to the skin formation.

To answer to these questions, we conducted experiments on the drying of two polymer solutions, polyvinyl acetate (PVAc) and polymethyl methacrylate (PMMA) in acetone. For these samples, we were able to take out the skin layer and measure its thickness and stiffness. We also observed the processes of formation and growth of the bubbles in such solution. By combining these information, we will answer the above questions for these systems.

2 Experiments

2.1 Samples

The polymers we used are poly-vinyl acetate (PVAc) and poly-methylmethacrylate (PMMA). They have similar chemical structure, but their glass transition temperatures T_g are considerably different. Their molecular weights are shown in table 1. Young's modulus in the table is Young's modulus of the skin layer obtained by the method described in sect. 2.4.

[a] e-mail: arai1010@iis.u-tokyo.ac.jp

Table 1. Samples.

	T_g (°C)	M_w (g/mol)	Young's modulus (Pa)
PMMA	104	996000	7×10^7
		120000	4×10^7
PVAc	28	500000	9×10^5
		113000	6×10^5

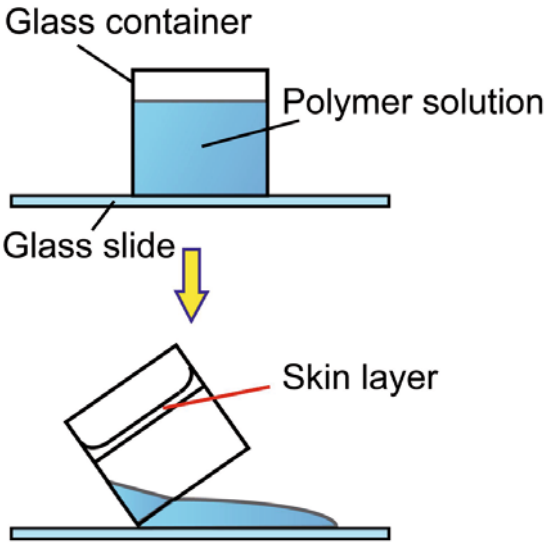

Fig. 1. The method of taking out the skin layer.

Acetone was used as solvent for both polymers. The initial concentration of the polymers was varied from 5 wt% to 40 wt%.

2.2 Drying experiment

The drying experiments were done in a cylinder (inner diameter 34.5 ± 1.5 mm, height 20 mm). The cylinder was placed on an electric balance and the weight of the sample was monitored during the drying experiment. The drying rate (g/min cm^2) was calculated from the loss of the weight per minutes divided by the cross-section of the cylinder.

2.3 Measurement of skins

The time variation of the thickness of the skin layers was obtained by the procedure shown in fig. 1. After the solution is dried for a certain period of time, the cylinder was tilted and the remaining liquid was poured out. When the skin layer is formed, a film remains at the top surface. The film was then dried, and the thickness of the dried film was measured by a micrometer.

This operation of taking out the skin layer was easy for the PMMA solution which forms stiff skin layers. For PVAc solution, it was difficult to take them out in the early stage as they are too soft to be taken out.

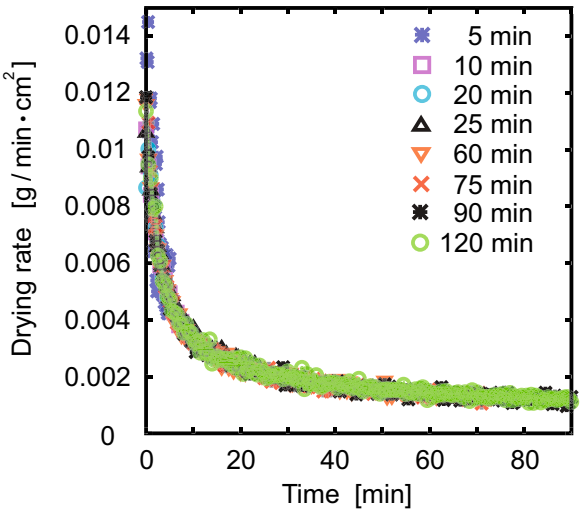

Fig. 2. Drying rate of PMMA solutions are plotted against the elapsed time for many experiments. The symbol "5 min" indicates the experimental result conducted to measure the skin thickness after 5 minutes.

The time dependence of the thickness of the skin layer was obtained by repeating the above experiments for many samples prepared and dried under the same condition. Utmost care is taken to ensure that the drying is done in the same condition. This was checked by measuring the drying speed. As is shown in fig. 2, we were able to reproduce the same drying speed for many experiments for the same solution. The crucial factor in getting such reproducibility was the height of the cylindrical container and the initial depth of the polymer solution. All experiments were done at room temperature (25 ± 1 °C).

Figure 3 shows the growth of the skin thickness for PMMA solution of molecular weight $M_w = 120000$. The skin layer was not formed for the first 45 minutes (meaning that all material flowed out when the container was tilted), but starts to appear around $t = 45$ min, and grows in time.

Figure 4 shows the growth of the skin layer for PMMA solution with high molecular weight ($M_w = 996000$). It is seen that the skin is formed shortly after the drying starts, and that the growth speed increases with the increase of initial polymer concentration.

2.4 Estimation of Young's modulus of skins

To estimate Young's modulus of the skins, we conducted the experiment shown in fig. 5. The polymer solution was dried in a rectangular trough. After the skins were formed, the bottom liquid was poured out, and the wet sides of the two skin layers were stuck together to make the specimen for the mechanical test. The elasticity of the specimen was measured by the stretching machine. The result are shown in table 1. The skin of PMMA solution is hard and glassy, while that of PVAc solution is quite soft.

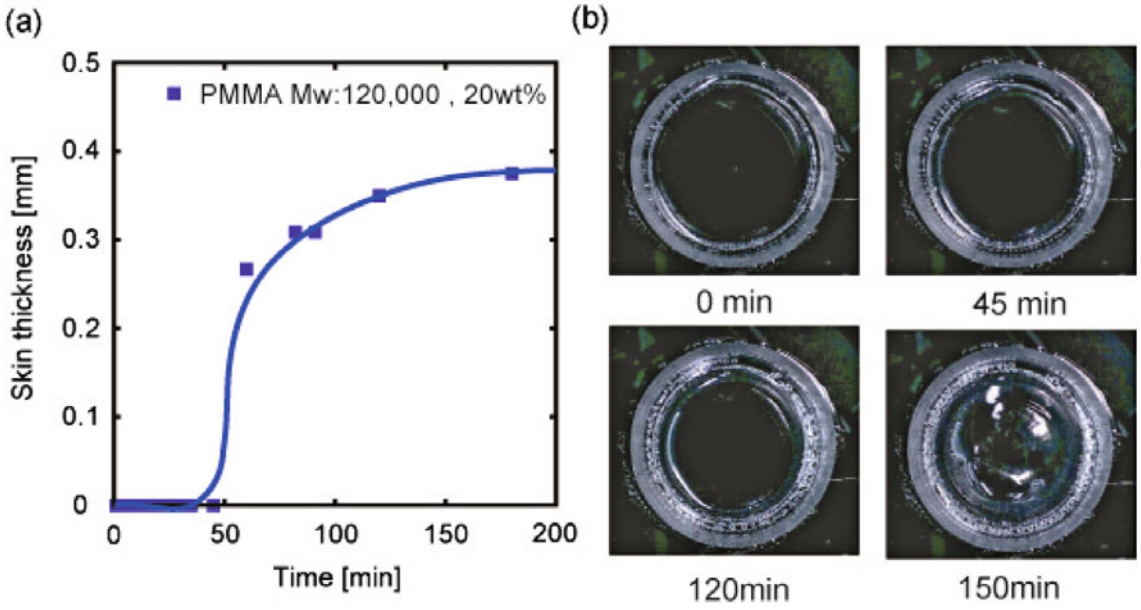

Fig. 3. (a) Thicknesses of skin layers for PMMA solution of M_w 120000 initial concentration 20 wt% is plotted against the elapsed time. (b) Top views of the sample.

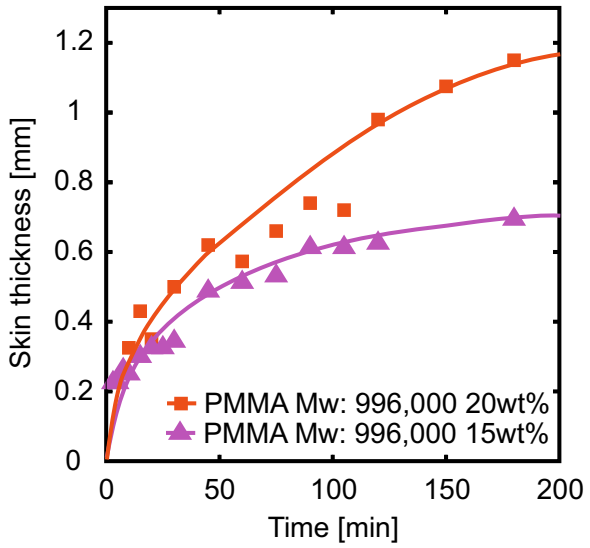

Fig. 4. Time dependence of the thickness of the skin layer of PMMA solution (M_w 996000) for two initial concentrations: 20 wt% and 15 wt%.

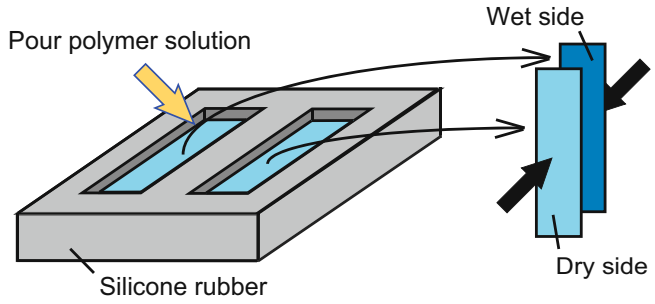

Fig. 5. The method of making samples to measure Young's modulus of skins.

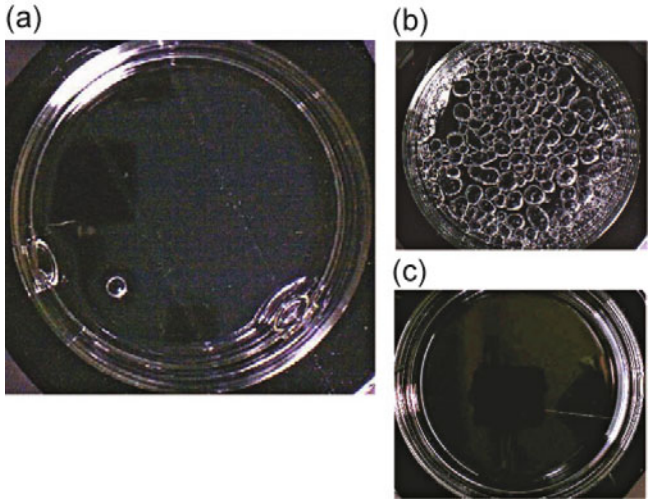

Fig. 6. Bubbles seen in the drying of PVAc/acetone solution ($M_w = 500000$, initial concentration 25 wt%) depend strongly on the evaporation rate. (a) An isolated bubble is seen at proper evaporation rate. (b) Many bubbles appear at fast evaporation rate. (c) No bubbles appear at slow evaporation rate. The evaporation rate is controlled by the wall height of the container.

2.5 Skin formation and bubble growth

Figure 3(b) shows the top views of the sample shown in fig. 3(a). For the first ca. 45 minutes, the sample looked the same as the initial solution, and the skin layer was not detected by the test explained in fig. 1. After an hour, the skin layer started to be seen. The formation of the skin layer was also seen by the deformation of the sample surface: before the skin was formed, the sample surface was flat, and the meniscus moved down uniformly. After

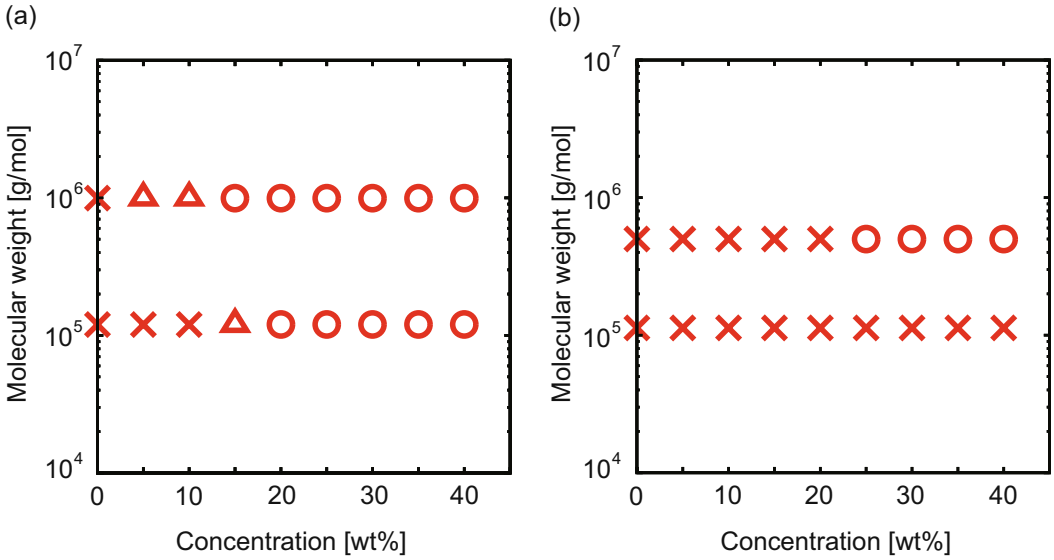

Fig. 7. Phase diagram for the bubble appearance; circle: bubbles always observed; cross: bubbles not observed; triangle: bubbles observed for some samples, but not for all samples. (a) PMMA/acetone solution; (b) PVAc/acetone solution.

the skin was formed, the surface started to curve since the outer edge of the surface was pinned to the wall container, while the central part of the surface kept moving down. After 2 hours later, bubbles were seen at the edge of the surface. As time went by, the surface became more curved, and the number of bubbles increased.

Similar phenomena are observed in other samples, but the appearance of the bubbles varied depending on the polymer, their molecular weight, and the initial concentration, etc. Figure 6(a) shows the bubbles formed in PVAc solution ($M_w = 500000$, 25%) dried in the same condition as the PMMA solution. In the PVAc solution, an isolated bubble is often seen when the drying was done in a mild condition. Such bubbles are suited for the study of bubble growth. If the drying speed is increased, many bubbles appear in the solution (see fig. 6(b)). If the drying speed is decreased (*e.g.*, by exposing the solution to solvent vapor), no skins and therefore no bubbles were seen.

We conducted the experiments by changing the molecular weight and concentration of the polymer, and checked whether the bubbles appear or not in the final sample. The results are summarized in fig. 7, where the circle indicates that the bubbles are formed, the cross indicates that no bubbles are formed, and the triangle indicates that the result depends on the samples. In the case of PMMA, bubbles are always seen at high concentration for both molecular weight. In the case of PVAc, bubbles are seen only for samples of high molecular weight and at high concentration.

These observations indicated that skin formation is a necessary condition for the bubble formation: Bubbles are not formed if skins are not formed. On the other hand, the skin formation does not necessarily lead to bubble formation. In certain conditions, bubbles were not observed for the samples which shows the skin formation.

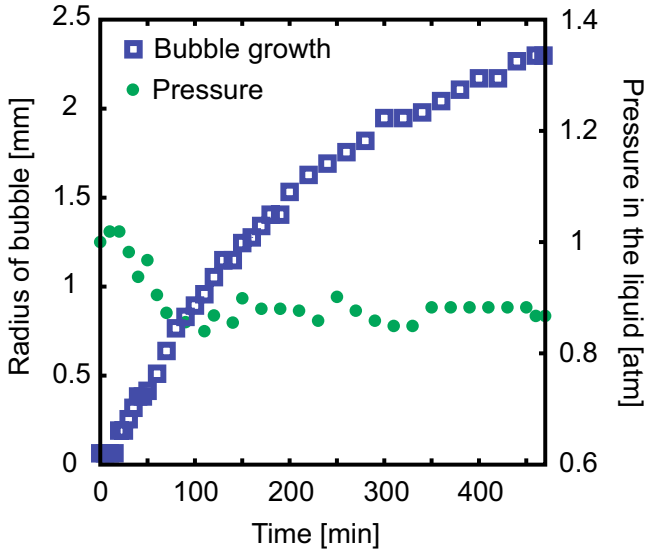

Fig. 8. Time dependence of the bubble radius, and the pressure of PMMA solution ($M_w = 996000$, initial concentration = 15 wt%).

2.6 Measurement of bubble growth

The time dependence of the bubble size was measured by the following procedure. We chose samples which contain an isolated bubble and obtained the time dependence of its radius from the area of the bubble image. Such measurement was not possible for all solutions. For some solutions, bubbles move toward the edge of the skin layer (due to the curve of the meniscus), and it was difficult to measure their size. In the PMMA solutions at high concentration, many bubbles appear and they coagulate to form a larger bubble. As a result the growth curves were

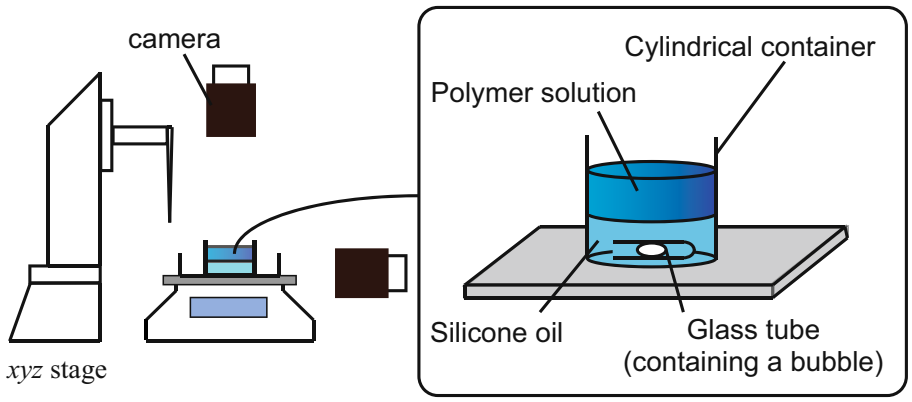

Fig. 9. Experimental setup to measure the pressure in the solution.

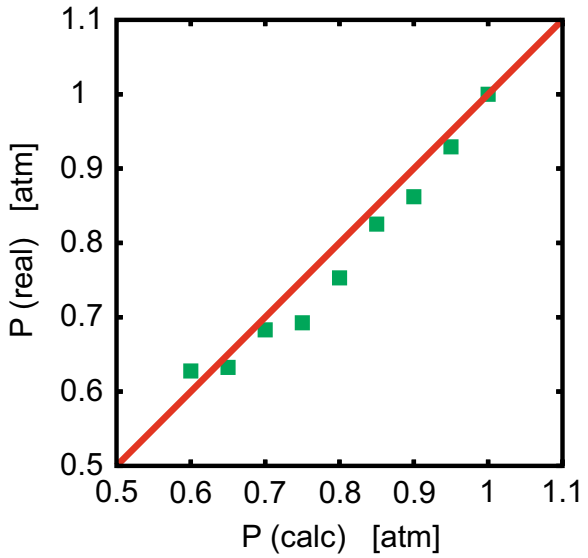

Fig. 10. Pressure calibration for the method shown in fig. 9.

obtained for limited cases, but they are sufficient to show the general trend in the bubble growth dynamics.

An example of the bubble growth in the PMMA solution is shown in fig. 8. In this case, the bubble appeared about 20 minutes after the start of the evaporation, and grew in time. The growth eventually stops when the solutions became glassy. The growth curves of other samples are shown later in the discussion section.

2.7 Measurement of the pressure change in the solution

The downward curving of the sample surface described in sect. 2.5 indicates that the pressure in the bulk liquid is less than the atmospheric pressure. To confirm this, we measured the pressure in the bulk liquid by the setup shown in fig. 9.

Silicone oil is first poured in the cylindrical container, and a glass tube which contains an air bubble is inserted. The polymer solution is then poured on top of the silicone oil. Due to the difference in the density, the polymer solution stays above the silicone oil as in fig. 9. In this set up, the silicone oil can be regarded as a pressure transmitter (the dissolution of polymer solution and the air into the silicone oil is negligible.) Therefore the pressure in the bulk solution can be obtained by measuring the volume of the air bubble. If the pressure in the bulk liquid decreases, the size of the air bubble increase. This is indeed seen in the drying of PMMA solution (see fig. 11(a)). It clearly indicates that the pressure in the bulk liquid indeed decreases in time.

The accuracy of this primitive pressure measurement is checked by placing the set up in a vacuum chamber, and compared the measured pressure with that indicated by the pressure meter in the vacuum chamber. The results agreed reasonably well as indicated by fig. 10.

Figure 11(b) shows the time variation of the pressure in the bulk liquid as the evaporation proceeds. In the case of PMMA solution, the pressure decreased by ca. 10% in the first 100 minutes, and stayed at constant value afterward. In the case of PVAc solution, the pressure did not change in a measurable amount. The reason for this will be discussed in the next section.

3 Discussion

3.1 Mechanism of the pressure decrease

The decrease of the pressure in the bulk liquid is considered to be caused by the mechanism explained in fig. 12. Once the surface is covered by the skin, further evaporation forces the skin to bend inward. This creates the restoring force F (see fig. 12) which is balanced by the pressure difference between the solution and the atmosphere.

The restoring force F can be estimated as follows. Let us assume that skin is an elastic plate having thickness h and Young's modulus E. If the center of the skin moves downward by d as in fig. 12, the strain of skin ϵ is estimated as $\epsilon \sim \frac{1}{2}\left(\frac{d}{L}\right)^2$, where L is the radius of the container.

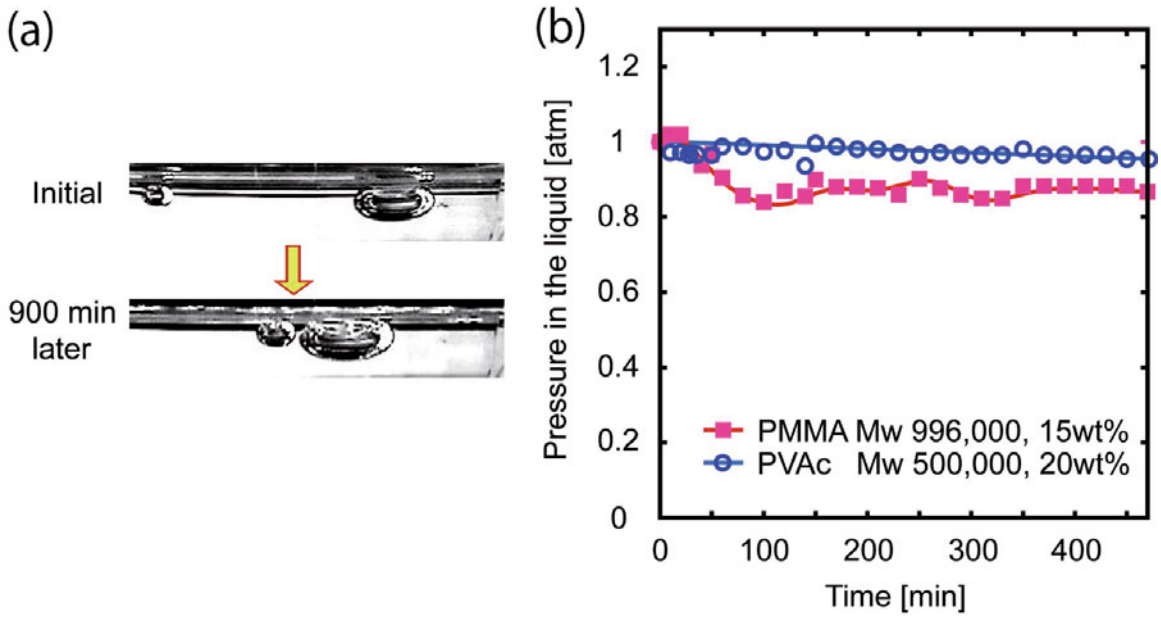

Fig. 11. (a) Growth of the air bubble trapped in the tube immersed in the silicone oil. (b) Time variation of the pressure in the solution.

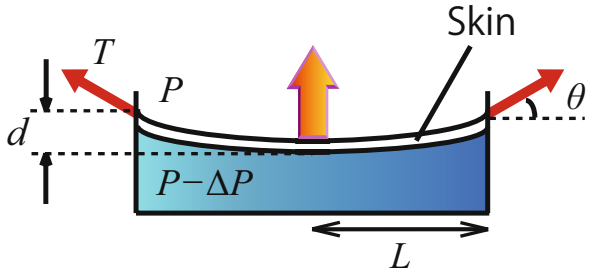

Fig. 12. Mechanism of the negative change of the pressure.

Hence F is written as

$$F \simeq 2\pi LEh\epsilon \sin\theta \simeq \pi L \cdot Eh \left(\frac{d}{L}\right)^2 \sin\theta \qquad (1)$$

and the pressure difference ΔP is estimated as

$$\Delta P \simeq \frac{F}{\pi L^2} = E\frac{h}{L}\left(\frac{d}{L}\right)^2 \sin\theta. \qquad (2)$$

With the values of E (shown in table 1), $\theta \approx 30°$, $h = 0.4\,\mathrm{mm}$, $d = 2\,\mathrm{mm}$, $L = 17\,\mathrm{mm}$, ΔP is estimated to be $10^4\,\mathrm{Pa}$ for PMMA and $10^2\,\mathrm{Pa}$ for PVAc. These values are in agreement with the experimental results shown in fig. 11(b). The reason that the pressure decrease was not observed for PVAc solution was that the skins were too soft to produce measurable pressure change. The stiffnesses of skins have an important role in changing the states of the bulk liquids.

3.2 Dynamics of the bubble growth

The pressure change is considered to be the cause of the bubble formation. As the pressure in the bulk liquid becomes less than the atmospheric pressure, the acetone in the solution will evaporate and form the bubbles. However, this simple interpretation is not totally consistent with our experimental observation.

1. Our experiment indicates that the pressure in the bulk liquid is 0.9 atm for PMMA and 1 atm for PVAc. This pressure is much larger than the vapor pressure of acetone, which is ca. 0.3 atm. The difference cannot be accounted for by the Laplace pressure which is at most 10^{-3} atm for a bubble of 1 mm.
2. As it is indicated in fig. 8, the bubble size is not directly coupled with the pressure change ΔP. Bubbles appear at a certain time after the skin is formed, and grow steadily even though the pressure remains constant.

These observations indicate that a significant part of the gas in the bubble is the air dissolved in the solution. Consider the bubble in PMMA/acetone solution. The pressure in the bubble is ca. 0.9 atm, but part of the pressure is due to the vapor pressure of acetone, which is 0.3 atm. The partial pressure of the air in the bubble is therefore 0.6 atm. Therefore the air in the bulk solution will evaporate into the bubble, and increase the volume of the bubble.

The equilibrium volume of the bubble (made of solvent and air) created in a bulk solution in a closed container can be calculated by using Henry's law. This is done in appendix A. In the case of PMMA solution, it is shown that the equilibrium volume is about one fourth of the bulk solution. The observed volume of the bubble is much less than this, but this is due to the solidification of the solution.

If the majority component of the bubble is the air, the growth of the bubble size should be governed by the diffusion of the air molecules (nitrogen and oxygen) in the

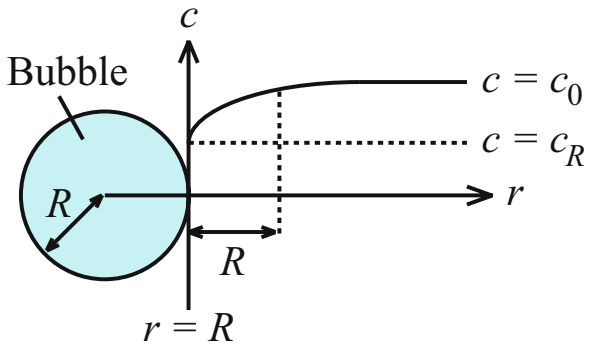

Fig. 13. Concentration profile of air components around the bubble.

bulk solution. (Such diffusion-limited growth of bubbles has been discuseed in geophysics [8,9].) Indeed, the observed growth law is consistent with this interpretation.

Consider an isolated bubble of radius R in the solution (see fig. 13). Let $c(r)$ be the weight of air dissolved in a unit volume at point r which is separated from the center of the bubble by the distance r. The time evolution of $c(r)$ is determined by the diffusion equation

$$\frac{\partial c}{\partial t} = D_p \nabla^2 c, \tag{3}$$

where D_p is the effective diffusion constant for air dissolved in the solution. At $r = R$, $c(r)$ is equal to the equilibrium value c_R: c_R is determined by the vapor pressure of acetone and the pressure in the bulk solution $P_0 - \Delta P$. At $r = \infty$, $c(r)$ is equal to c_0, the value in the original solution. Since c_0 is larger than c_R, the air diffuses in the solution toward the bubble.

Since the change of the bubble radius R takes place very slowly, we may solve eq. (3) using the steady-state approximation, $\nabla^2 c = 0$. The solution of this equation is

$$c(r) = c_R + \left(1 - \frac{R}{r}\right)(c_0 - c_R). \tag{4}$$

Therefore the flux of the air diffusing into the bubble per unit time is

$$J = -D_p \left(\frac{\partial c}{\partial r}\right)\bigg|_{r=R} = D_p \frac{c_0 - c_R}{R}. \tag{5}$$

The mass balance of the solvent and air is written as follows:

$$\frac{\mathrm{d}}{\mathrm{d}t}\left(\frac{4}{3}\pi\rho_g R^3\right) = 4\pi R^2 J, \tag{6}$$

where ρ_g is the density of the gas in the bubble (we have ignored the contribution of acetone evaporation). Equations (5) and (6) give the following time evolution equation for R:

$$\frac{\mathrm{d}R}{\mathrm{d}t} = \frac{(c_0 - c_R)D_p}{\rho_g R}, \tag{7}$$

which is easily solved as

$$R = \left(2\frac{(c_0 - c_R)D_p}{\rho_g}(t - \tau)\right)^{1/2}, \tag{8}$$

where τ is the time at which the bubble starts to appear. This time is called the induction time.

Equation (8) is compared with the experimental results in fig. 14. Figure 14(a) shows the case of PMMA solution (M_w: 996000, 15 wt%) and (b) shows the case of PVAc solution (M_w: 500000, 25 wt%). It is seen that the agreement between the observed curve and the theoretical curve is good.

The induction time is quite different for two solutions ($\tau = 180\,\mathrm{min}$ for PVAc solution, and $\tau \simeq 20\,\mathrm{min}$ for PMMA solution), but the coefficients $(c_0 - c_r)D_p/\rho_g$ are similar to each other. The difference in the induction time can be explained by the difference in the pressure change ΔP. The PMMA solution has a stiff skin layer, and large pressure change, while the PVAc solution has soft skin layer, and small pressure change. This makes the large difference in the induction time for the two solutions. On the other hand, the coefficients are not very much different since the parameters c_0, c_R, D_p are essentially determined by acetone and air, and will not depend on the solute polymer.

Figure 15 shows the plot of $R(t)$ against $t - \tau$ for many samples. The filled marks indicate the PVAc solutions, and the open marks indicate the PMMA solution. It is seen that the growth of the bubble size is essentially described by eq. (8) for all samples.

4 Conclusion

We have shown that the bubbles seen in the drying polymer solution (PMMA/acetone and PVAc/acetone) are the mixture of acetone vapor and air coming from the solution. The bubble formation is closely related to the skin formation. Our experiment indicates the following scenario for the bubble formation.

Dimple formation?

1. First, the skins are formed at the surface of the polymer solution. Further evaporation of the solvent deforms the skin layer since the edge of the skin is fixed to the wall of the container. The elastic restoring force of the skin layer gives a negative change in the pressure in the solution, and assists the nucleation of bubbles.
2. Once bubbles nucleate, air tends to diffuse from the solution to the bubble since the partial pressure of air in the bubble is less than the atmospheric pressure. The growth rate of the bubble is dominated by the diffusion of the air. Degas polymer solution first?
3. As the solvent evaporates further, the viscosity of the polymer solution increases, and the system solidifies. The bubbles are then trapped in the final product.

This scenario is consistent with our experimental observations: i) The induction time of PMMA/acetone solution is much less than that of PVAc/acetone solution, since the pressure change in PVAc solution is much less than that of PMMA solution. ii) The bubble size increases in proportion to the square of the elapsed time. Direct confirmation of our scenario may be possible by analyzing the gas in the bubble, and/or by using a slippery wall which does not pin the skin layer. This will be a future work.

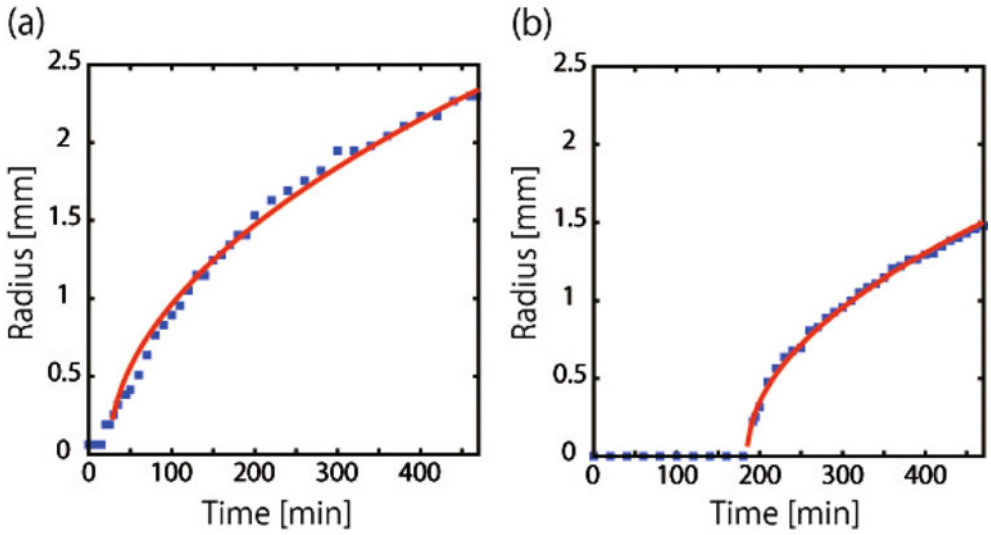

Fig. 14. (a) Time dependence of the size of an isolated bubble formed in PMMA solution ($M_w = 996000$, initial concentration 15%). The symbols indicate the experimental value and the solid line indicates the theoretical curve (eq. (8)). (b) The same for PVAc solution ($M_w = 500000$, initial concentration 40%).

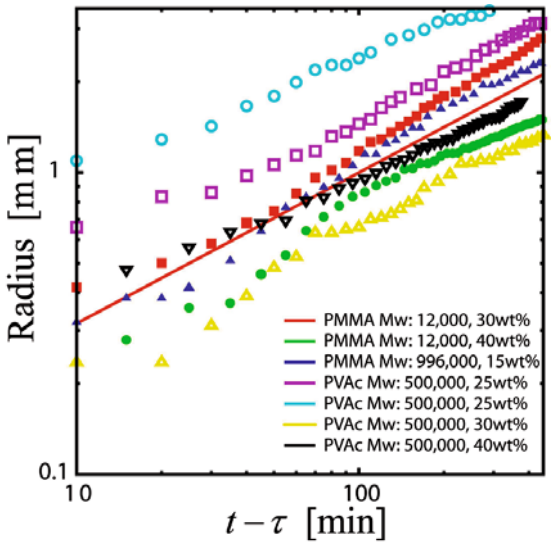

Fig. 15. The radii of isolated bubbles are plotted against the elapsed time since their appearance.

The authors are grateful to Y. Sumino and T. Kajiya for their interest in this subject and their useful suggestions.

Appendix A. The air in the bubbles

We will calculate the equilibrium volume of the bubble (*i.e.*, the gas phase) in the PMMA/acetone solution for the following idealized situation. The solution is assumed to be in the container of fixed volume V_0. Initially, the solution occupies the whole volume V_0 under pressure P_0. The amount of air dissolved in the solution is given by Henry's law

$$w_0 = \alpha P_0 V_0, \tag{A.1}$$

where α is Henry's constant. Suppose that a fraction of the solution is extracted from the system, and the pressure of the container is changed from P_0 to $P = P_0 - \Delta P$. Then the solvent and the air evaporate and form the bubble. We will calculate the volume of the bubble at equilibrium.

The partial pressure of acetone in the bubbles is the saturated vapor pressure P_{ace} The partial pressure of air in the bubble is therefore

$$P_b = P_0 - \Delta P - P_{\mathrm{ace}}. \tag{A.2}$$

Let V_b be the volume of the bubble, and w_b be the weight of the air in the bubble. They are related by the equation of state of gas

$$P_b = \frac{w_b RT}{MV_b}, \tag{A.3}$$

where M is the effective molecular weight of the air. On the other hand, Henry's law is written as

$$w_0 - w_b = \alpha P_b (V_0 - V_b). \tag{A.4}$$

Equations (A.2)-(A.4) give

$$V_b = \frac{P_0 - P_b}{P_b} \cdot \frac{1}{\frac{1}{\beta} - 1} V_0, \tag{A.5}$$

where $\beta = \alpha RT/M$ is the Ostwald number.

According to [10] the Ostwald number β of air in acetone is 0.2 (at 25 °C). This gives $V_b \approx 0.17 V_0$. This is the equilibrium volume of the bubble. The value corresponds to the upper limit of bubble volume. In the situation of our experiment, the system is not in equilibrium: the solvent keeps evaporating and solidification takes place. The above analysis indicates that the volume of the air coming from the solution is significantly large, and supports our argument that the significant amount of the gas in the bubble is air.

References

1. P.G. de Gennes, Eur. Phys. J. E **7**, 31 (2002).
2. T. Okuzono, K. Ozawa, M. Doi, Phys. Rev. Lett. **97**, 136103 (2006).
3. L. Pauchard, C. Allain, Europhys. Lett. **62**, 897 (2003).
4. L. Pauchard, C. Allain, C.R. Physique **4**, 231 (2003).
5. T. Kajiya, E. Nishitani, T. Yamaue, M. Doi, Phys. Rev. E **73**, 011601 (2006).
6. R.D. Deegan, O. Bakajin, T.F. Dupont, G. Huber, S.R. Nagel, T.A. Witten, Nature (London) **389**, 827 (1997).
7. Y. Shimokawa, T. Kajiya, K. Sakai, M. Doi, Phys. Rev. E **84**, 051803 (2011).
8. A.A. Prousevitch, D.L. Sahagian, A.T. Anderson, J. Geophys. Res. B **98**, 22283 (1993).
9. A.A. Prousevitch, D.L. Sahagian, J. Geophys. Res. B **103**, 18223 (1998).
10. C.B. Kretschmer, J. Nowakowska, R. Wiebe, Ind. Eng. Chem. **38**, 506 (1946).